⌘ *Author's Choice*

THE JOURNAL OF BIOLOGICAL CHEMISTRY VOL. 287, NO. 22, pp. 18730–18737, May 25, 2012

Characterization of Chromoshadow Domain-mediated Binding of Heterochromatin Protein 1α (HP1α) to Histone H3*[S]

Received for publication, December 22, 2011, and in revised form, March 23, 2012 Published, JBC Papers in Press, April 9, 2012, DOI 10.1074/jbc.M111.337204

Alexandria N. Richart, Clair I. W. Brunner, Katherine Stott, Natalia V. Murzina[1], and Jean O. Thomas[2]

From the Department of Biochemistry, University of Cambridge, Cambridge CB2 1GA, United Kingdom

Background: Heterochromatin protein 1 (HP1) is a non-histone chromatin protein that interacts with histone H3 through both the chromodomain and chromoshadow domain.
Results: The chromoshadow domain specifically interacts with H3 residues located inside the nucleosome, close to the dyad.
Conclusion: Rearrangement of the nucleosomal DNA is a prerequisite for binding.
Significance: This interaction provides new insight into the structure of silenced chromatin.

The chromoshadow domain (CSD) of heterochromatin protein 1 (HP1) was recently shown to contribute to chromatin binding and transcriptional regulation through interaction with histone H3. Here, we demonstrate the structural basis of this interaction for the CSD of HP1α. This mode of H3 binding is dependent on dimerization of the CSD and recognition of a P*x*V*x*L-like motif, as for other CSD partners. NMR chemical shift mapping showed that the H3 residues that mediate the CSD interaction occur in and adjacent to the αN helix just within the nucleosome core. Access to the binding region would require some degree of unwrapping of the DNA near the nucleosomal DNA entry/exit site.

Heterochromatin protein 1 (HP1)[3] is a highly conserved and abundant non-histone chromosomal protein. It participates in gene silencing and in transcriptional activation (reviewed in Refs. 1–3) and is also implicated in DNA repair (4). Fluorescence recovery after photobleaching measurements on GFP-HP1 show that HP1 binding to chromatin is dynamic and that HP1 is less mobile in heterochromatin than in euchromatin (5–8).

HP1 exists in mammals as three isoforms (α, β, and γ), which have high sequence homology and similar structures. HP1α is found mostly in cytologically dense heterochromatin, whereas HP1β and HP1γ are also found in euchromatin. The isoforms are all homodimers in which the monomeric unit comprises (i) a chromodomain (CD), which specifically recognizes the methylation mark at di- and trimethylated H3K9 (9, 10); (ii) a flexible interdomain hinge region of variable sequence and length, which contains a putative KRK nuclear localization signal and has been shown to bind DNA (11); and (iii) a chromoshadow domain (CSD), which mediates dimerization of HP1 and recruitment of a variety of other nuclear chromatin-modifying proteins (12), many of which contain a P*x*V*x*L motif (13, 14). The CD and CSD have high amino acid sequence homology and very similar folds (15, 16). HP1 is generally believed to cause gene repression through chromatin compaction (17, 18), mostly in H3K9-methylated regions (19). However, it also condenses reconstituted chromatin arrays in the absence of H3K9 methylation (20), suggesting an additional methylation-independent structural role of HP1 in chromatin compaction and repression. (Dimerization of CD sticky ends on two adjacent HP1 molecules has been suggested as one possible mechanism (21).)

The CSD appears to interact directly in an H3K9 methylation-independent manner with a region at the edge of the histone H3 globular domain, which contains a P*x*V*x*L motif (see Fig. 1*A*), suggested to be the binding site (22). Phosphorylation of Tyr-41 within this region leads to displacement of HP1α from heterochromatin (23). The structural basis of CSD dimer binding to other proteins containing a P*x*V*x*L motif has been determined (24, 25).

We confirm here a role for P*x*V*x*L-mediated recognition of H3 by the CSD of HP1α (CSDα). We demonstrate a requirement for CSD dimerization, and using NMR, we identify the residues that mediate the interaction. The CSD dimer specifically interacts with the H3 residues just within the nucleosome, including (part of) the αN helix, close to the DNA entry/exit sites. This provides a second component to the interaction of HP1α with H3, in addition to the methylation-dependent interaction with di- or trimethylated H3K9 via the CD.

EXPERIMENTAL PROCEDURES

Protein Expression and Purification—Human histone H3(1–59) was expressed from plasmid pGEX2TL-H3(1–59), and human HP1 CSDα (109–185) was expressed from pGEX2T-

* This work was supported by Project Grant 094519/Z/10/Z from the Wellcome Trust (to J. O. T. and N. V. M.) and by a scholarship from the Gates Cambridge Trust (to A. N. R.).
⌘ *Author's Choice*—Final version full access.
[S] This article contains supplemental Fig. 1.
The chemical shift assignments have been deposited in the Biological Magnetic Resonance Data Bank under BMRD accession numbers 18385 and 18386.
[1] To whom correspondence may be addressed. Tel.: 44-1223-764826; Fax: 44-1223-766002; E-mail: nm@mole.bio.cam.ac.uk.
[2] To whom correspondence may be addressed. Tel.: 44-1223-333670; Fax: 44-1223-766002; E-mail: jot1@cam.ac.uk.
[3] The abbreviations used are: HP1, heterochromatin protein 1; CD, chromodomain; CSD, chromoshadow domain; CSDα, CSD of HP1α; HSQC, heteronuclear single quantum coherence; TOCSY, total correlation spectroscopy; CSDβ, CSD of HP1β.

HP1CSDα(109–185) (a gift from Dr. A. Bannister). GST-H4(1–48) was produced as described by Verreault *et al.* (26), GST-CAF1 p150(176–327) as described by Murzina *et al.* (13), and CAF1 p150(210–238) as described by Thiru *et al.* (24). CSDα point mutations (I165E, W174A, and E179*X*) and a stop codon at residue 60 in histone H3 (to generate pGEXTL-H3(1–59) from pGEXTL-H3(1–135) (26)) were introduced using a QuikChange II site-directed mutagenesis kit (Stratagene) according to the manufacturer's instructions.

All proteins were expressed as GST fusions in *Escherichia coli* Tuner(DE3)pLacI cells (Novagen) in 2× TY (Tryptone and yeast extract) medium at 20 °C. ^{15}N-Labeled H3(1–59) was produced in M9 minimal medium, and uniform ^{15}N labeling was achieved using [^{15}N]NH_4Cl as the sole nitrogen source for bacterial growth. ^{15}N-Labeled CSDα(109–185) was expressed in MOPS minimal medium containing [^{15}N]NH_4Cl and 0.25 g/liter ^{15}N-labeled ISOGRO® powder (Sigma-Aldrich) as nitrogen source. The proteins were affinity-purified on glutathione-Sepharose beads (GE Healthcare) using standard protocols. The GST tag was left intact for *in vitro* binding (pulldown) assays, but for NMR experiments, it was removed with thrombin (Novagen). ^{15}N-Labeled H3(1–59) was further purified on a Mono S column (GE Healthcare). ^{15}N-Labeled CSDα(109–185) was purified on Mono Q and then Superdex 75 gel filtration columns (GE Healthcare).

GST Pulldown Assays—Approximately 5 μg of protein was mixed with a GST fusion protein immobilized on glutathione-Sepharose beads in 250 μl of binding buffer (150 mM NaCl, 20 mM Tris-HCl (pH 7.5), 5 mM DTT, 0.25% Nonidet P-40, and 1× complete protease inhibitor mixture (Roche Applied Science)). 25% of the mixture was kept separately as the input sample. After incubation at 4 °C for 2 h, the beads were washed four times with 0.7 ml of binding buffer. Bound proteins were eluted from the beads with SDS-PAGE loading buffer (Invitrogen), separated on 12% NuPAGE (Invitrogen) precast gels, and stained with Instant Blue (Expedeon Protein Solutions).

NMR Spectroscopy—NMR measurements were made on ^{15}N-labeled proteins (0.2–0.5 mM) in 10% D_2O, 10 mM sodium phosphate (pH 7.0 for ^{15}N-labeled H3(1–59) and pH 8.0 for ^{15}N-labeled CSDα(109–185)), 1 mM EDTA, 1 mM DTT, 1× protease inhibitor mixture (0.05 mg each of leupeptin, aprotinin, and pepstatin A and 78 mg of benzamidine per 10 ml for a 50× stock), and 100 μg/ml 1-chloro-3-tosylamido-7-amino-2-heptanone. Experiments were recorded at 25 °C (for ^{15}N-labeled CSDα) or 0 °C (for ^{15}N-labeled H3) on a Bruker DRX600 spectrometer. Data were processed using the Azara suite of programs (version 2.8). Backbone assignments were made in three-dimensional NOESY-^{15}N heteronuclear single quantum coherence (HSQC) and total correlation spectroscopy (TOCSY)-^{15}N HSQC experiments (27) using CcpNmr Analysis version 2.1 (28). Chemical shift differences were calculated using $\Delta\delta = ((\Delta\delta^{H})^2 + (0.15 \times \Delta\delta^{N})^2)^{1/2}$ (29).

Fluorescence Spectroscopy—The binding of increasing concentrations of the CAF1 peptide to 300 nM CSDα dimer in 10 mM sodium phosphate (pH 8.0) was measured using fluorescence emission at 350 nm (PerkinElmer LS55 spectrofluorometer) with an excitation wavelength of 280 nm, at 25 ± 0.1 °C.

Affinity Measurements—K_D values were calculated from fitting the NMR and fluorescence data to $\Delta = \Delta_\infty(-([\text{CSD}\alpha] + [x] + K_D) - \sqrt{([\text{CSD}\alpha] + [x] + K_D)^2 - (4[\text{CSD}\alpha][x])})/2[\text{CSD}\alpha]$, where *x* denotes either the H3 or CAF1 peptide, and Δ is either the chemical shift difference or the change in intrinsic tryptophan fluorescence on addition of H3 or CAF1, respectively. (Representative fits are shown in supplemental Fig. 1.) The reported K_D was obtained by averaging the fitted values from three different residues (Ile-113, Gly-116, and Asp-149) for NMR or over three repeat measurements for fluorescence. In fitting the NMR data, [CSDα] (116 μM dimer) and [H3] (23–464 μM) were adjusted for dilution effects; dilution had a minimal effect on the CSDα intrinsic fluorescence, as the final volume increase was below 5%.

RESULTS

Dimerization of CSDα Is Required for H3(1–59) Interaction—The reported interaction between CSDα and H3 was demonstrated using a pulldown assay with a GST-tagged H3 peptide (residues 1–59) (Fig. 1*A*) containing the part of the H3 tail that protrudes from the nucleosome (residues 1–38), followed by the residues (residues 39–43) that pass between the DNA gyres and then the αN helix (residues 45–56), which is located within the nucleosome core (30). This region of H3 contains a variant of the P*x*V*x*L motif, ^{43}*P*GT*VAL*^{48}. The binding of CSDα to GST-H3(1–59) and CAF1 p150(176–327), which contains a well characterized P*x*V*x*L motif (13), was compared in a pulldown assay. The result (Fig. 1*B*) confirms the reported interaction of H3 with CSDα and indicates that H3 interacts less strongly than CAF1 (compare *lanes 8* and *14*); an H4 peptide containing residues 1–48 did not interact in this experiment (*lane 11*).

The role of the H3 P*x*V*x*L-like motif in binding to CSDα was investigated further by mutagenesis of key residues, identified based on those involved in the well characterized interaction of the CSD of HP1β (CSDβ) with the CAF1 p150 P*x*V*x*L peptide. This binds to the CSD across the dimer interface (13, 16, 24); the dimeric structure is also required for the interaction of HP1 with H3 because mutation of Ile-165, a key dimerization residue in CSDα, to glutamic acid (mutant I165E) abolished the interaction with H3(1–59) (Fig. 1*C*). Trp-170 has previously been shown to be critical for the CSDβ interaction with P*x*V*x*L motif-containing proteins (16, 24), and the corresponding residue, Trp-174, is important in the interaction of CSDα with GST-H3(1–59) because the interaction was abolished in mutant W174A (Fig. 1*C*). These results therefore suggest a role in CSDα recognition for the P*x*V*x*L-like motif in H3(1–59). In addition, a CSDα C-terminal tail deletion mutant, E179*X*, in which Glu-179 was replaced with a stop codon, had no effect on the interaction of CSDα with GST-CAF1 p150(176–327), whereas it significantly reduced the interaction with GST-H3(1–59) (Fig. 1*C*), indicating that the HP1α unstructured C-terminal tail plays a role in the interaction with H3.

CSDα Interacts Similarly with H3(1–59) and a PxVxL-containing Peptide—As a prelude to NMR chemical shift perturbation mapping to identify the CSDα(109–185) residues involved in the interaction with H3(1–59), we assigned the $^{1}H^{N}$ and ^{15}N

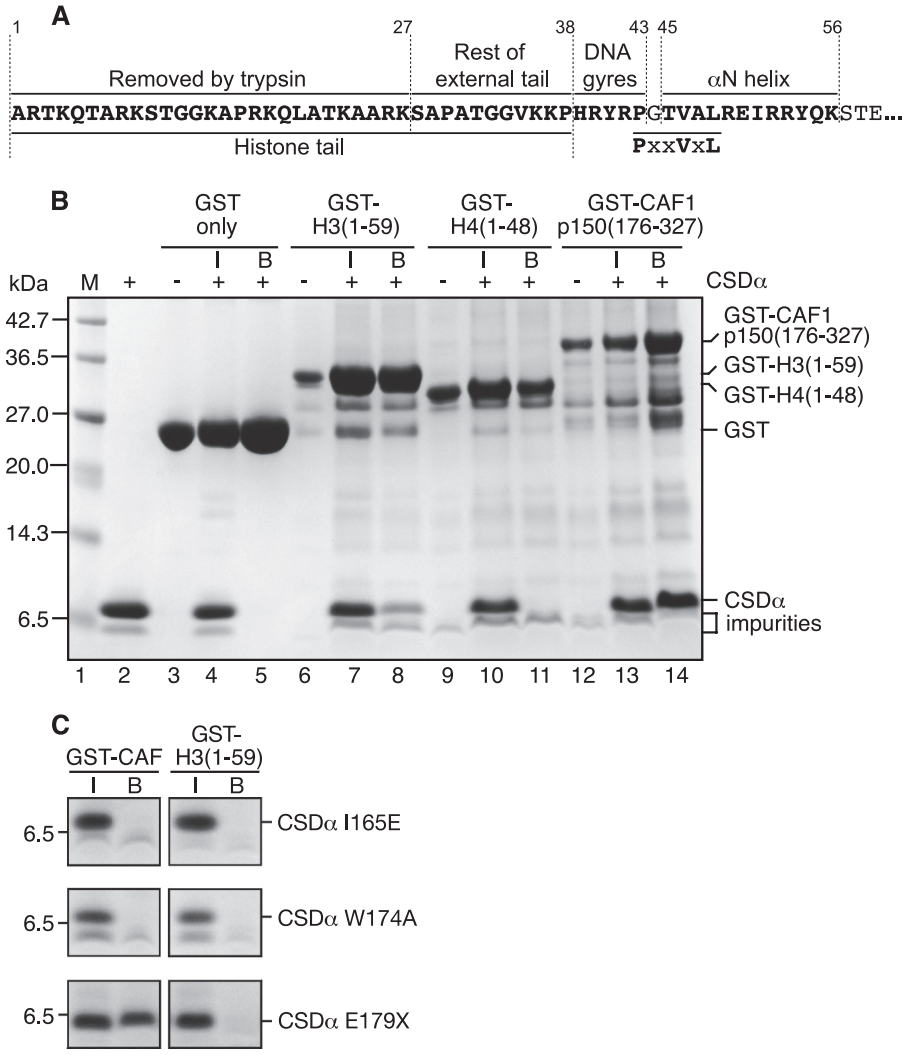

FIGURE 1. **Comparison of wild-type and mutant CSDα binding to H3(1–59) and P*x*VxL-containing CAF1 p150(176–327) peptide.** *A*, sequence of H3(1–59) showing the exposed and buried regions in the context of the nucleosome and the positions of the αN helix and the PxVxL-like motif. *B* and *C*, pulldown of wild-type and mutant CSDα, respectively, with GST fusion peptides immobilized on glutathione-Sepharose beads. *I*, input with 25% of total proteins; *B*, bound proteins, left on the beads following washing; *M*, protein molecular mass markers (broad range, New England Biolabs).

amide resonances of ^{15}N-labeled CSDα using three-dimensional NOESY-^{15}N HSQC and TOCSY-^{15}N HSQC experiments (27). All but four of the non-proline residues could be assigned in the structured region (residues 114–174); residues at the N and C termini were often broad and/or overlapped such that only very few could be assigned unambiguously. ^{15}N HSQC spectra of ^{15}N-labeled CSDα alone and in the presence of H3(1–59) at H3(1–59):^{15}N-labeled CSDα dimer molar ratios of 0.6:1, 1:1, and 4:1 are shown in Fig. 2*A*. Some peaks did not shift upon addition of H3(1–59) (*e.g.* Gly-120 and Cys-160) as shown in expansions of the spectra in Fig. 2*B*. Others (*e.g.* Asp-149 and Val-151) showed significant progressive shifts, indicative of fast exchange on the chemical shift time scale. Several others shifted to a larger extent and became increasingly broad as the resonances approached the intermediate chemical exchange regime. For many of this latter set (*e.g.* Trp-174, Ser-132, and Gly-134), the final peak is split into two separately identifiable resonances, indicative of a breakdown in the symmetry of the CSDα dimer on binding the H3 peptide, as was seen previously in studies of the complex of the CSDβ dimer with the CAF1 peptide containing a P*x*V*x*L motif (24). For comparison, ^{15}N HSQC experiments with CSDα in the presence of the CAF1 peptide were also recorded at a range of molar ratios (Fig. 2*C*). Comparison of the CSDα/H3 and CSDα/CAF1 perturbations revealed that the same CSD resonances responded to both CAF1 and H3. The main difference was that slightly larger shifts were seen for the CAF1 peptide, and saturation was achieved at a lower ratio. This suggests that the H3 and CAF1 peptides recognize the same binding interface on CSDα, but H3 has a significantly lower affinity.

An average K_D for the H3/CSDα interaction of 58 $\pm$ 7 μM was obtained from the NMR data using the resonances that were in fast exchange (supplemental Fig. 1*A*). This was not possible for CAF1 because most peaks showed signs of broadening due to intermediate exchange. However, a K_D of 0.43 $\pm$ 0.10 μM was obtained from intrinsic tryptophan fluorescence measurements (supplemental Fig. 1*B*). (Isothermal titration calorimetry proved unsuitable due to very low enthalpies for the CAF1/CSDα interaction.)

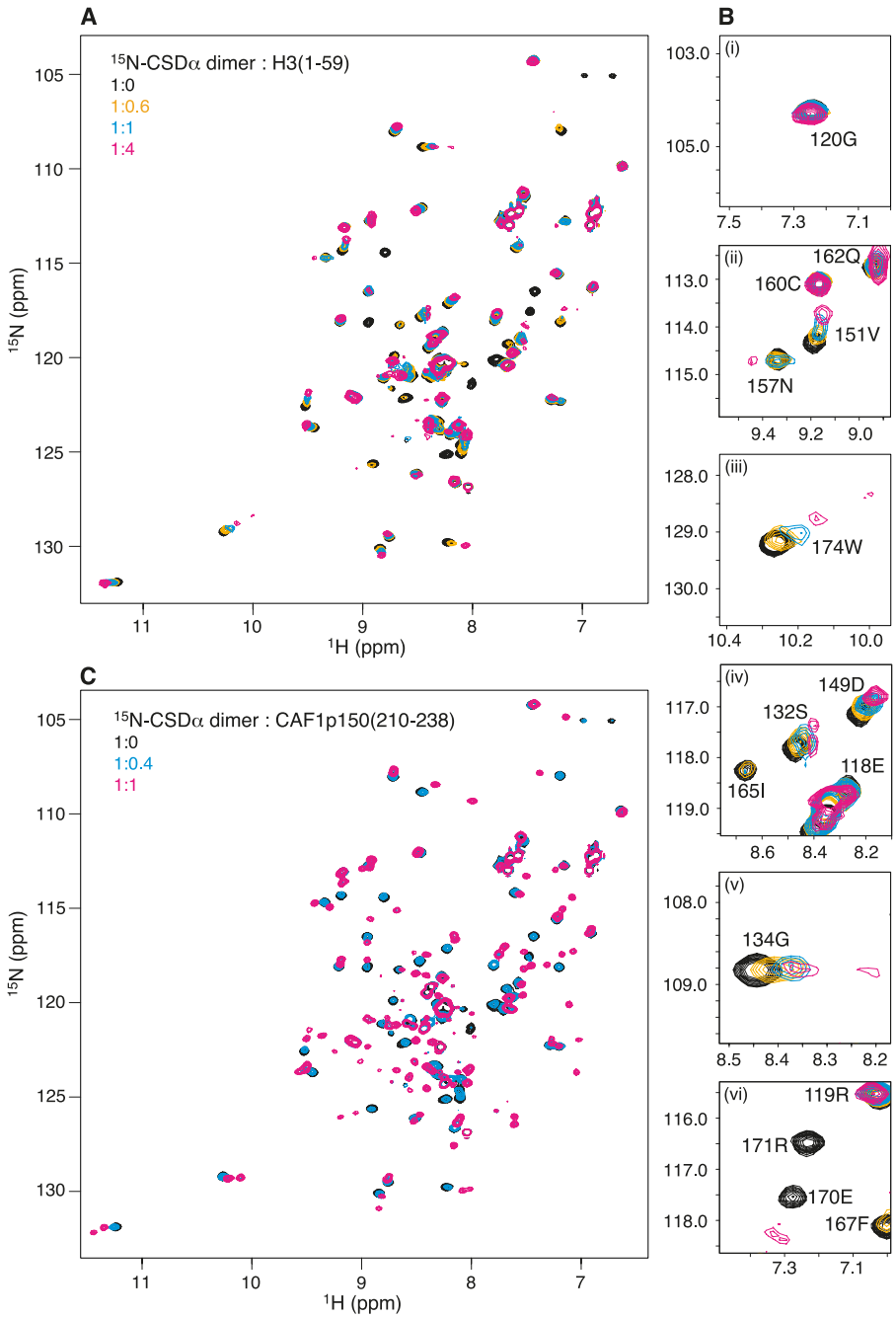

FIGURE 2. **Comparison of interactions of CSDα with H3(1–59) and CAF1 p150(210–238) peptides by NMR.** *A*, ^{15}N HSQC spectra of CSDα (*black*) titrated with H3(1–59) at the input ratios of CSD dimer to peptide monomer indicated. *B*, expanded views of peaks that exemplify different behavior: unperturbed (*panel i*), shift (*panel ii*), shift and split (*panels iii–v*), and disappearance (*panel vi*), on addition of H3(1–59). *C*, spectra of ^{15}N-labeled CSDα titrated with the CAF1 peptide showing a broadly similar response for comparison.

The perturbations in the NMR spectra of CSDα/CAF1 closely resembled those recorded for CSDβ in the presence of the CAF1 peptide (24), suggesting identical interaction of the α- and β-isoforms with CAF1 p150. In many cases, peak doubling or peak broadening/disappearance prevented the precise quantification of chemical shift changes. Therefore, a qualitative assessment of each peak was made for both the CAF1 and H3(1–59) titrations, and where possible, peaks were classed according to one of four specific behaviors: no shift, small shift, large shift and/or doubling, and disappearance/ambiguous. The peak behavior for each residue of CSDα upon titration with either H3(1–59) or the CAF1 peptide was mapped onto the structure of highly homologous CSDβ, as the only available CSDα structure (CBX5; Protein Data Bank code 3I3C) lacks the peptide substrate, and the interacting region is disordered (Fig. 3). Where it was possible to assign peaks and their shifts, it was clear that binding of H3(1–59) to CSDα produced a pattern of peak shifts/peak doubling similar to that for binding of the CAF1 peptide, confirming that the binding interfaces for H3 and CAF1 on CSDα overlap. A few residues farther away from the P*x*V*x*L-binding site were affected by CAF1 binding, but not by H3 binding.

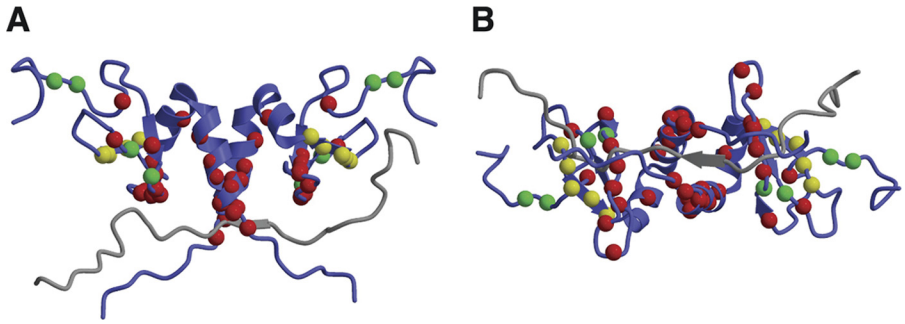

FIGURE 3. **Comparison of H3(1–59)- and CAF1 p150(210–238)-binding sites on CSD.** *A*, qualitative comparison of the H3(1–59)- and CAF1 peptide-binding sites mapped onto a structure of the homologous CSDβ dimer-CAF1 peptide complex (Protein Data Bank code 1S4Z (24)), with CSDβ in *purple ribbons* and CAF1 in *gray*. Residues displaying a large chemical shift change in both the H3(1–59) and CAF1 complexes are shown in *red* (space filling). Residues that shift to a lesser extent in both complexes are shown in *yellow*; residues that shift with the CAF1 peptide only are shown in *green*. *B*, same as *A* after a 90° rotation about the horizontal axis. Structural representations were prepared using MolScript (31) and Raster3D (32).

Residues 36–58 of H3(1–59) Interact with CSDα—To map precisely the binding site for CSDα on H3(1–59) using ^{15}N HSQC chemical shift perturbation experiments, all non-proline $^{1}H^{N}$ and ^{15}N amide resonances of ^{15}N-labeled H3(1–59) were first assigned using three-dimensional NOESY-^{15}N HSQC and TOCSY-^{15}N HSQC experiments (27). Elevated $\{^{1}H\}^{15}N$ heteronuclear NOE values measured for free H3(1–59) indicated that residues 39–55 are partially structured in the free peptide (Fig. 4*C*). These residues coincide with the αN helix seen in the context of the nucleosome, but also extend ~6 residues to the N-terminal side of this region. Spectra of ^{15}N-labeled H3(1–59) alone, and in the presence of CSDα at molar ratios of 0.5:1, 1:1, and 3.6:1 CSDα dimer:^{15}N-labeled H3(1–59), are shown in Fig. 4*A*. Although some perturbed residues were in the fast exchange regime and therefore trackable by their progressive changes in chemical shift, the peaks corresponding to residues 37–56 disappeared entirely upon the first addition of CSDα (0.5:1 molar ratio) and did not reappear with further addition, even at a 3.6-fold excess of the CSDα dimer to the H3 peptide. Expanded views (Fig. 4*B*) highlight residues that disappeared entirely (*e.g.* Arg-42) or shifted progressively (*e.g.* Lys-36 and Thr-58) on addition of CSDα. The ^{1}H and ^{15}N chemical shift differences were scaled appropriately, combined (as $\Delta\delta$) (29), and plotted in Fig. 4*C*. This shows that residues that disappeared, shown as "quenched peaks," are flanked on either side by the residues that show the largest trackable perturbations, suggesting that the whole of the region comprising H3(36–58) is involved in the interaction with CSDα. Identical results were obtained when analogous titrations were performed with CSDβ and ^{15}N-labeled H3(1–59) (data not shown). The interacting region of H3 (residues 36–58) encompasses the segment that exits the nucleosome through the aligned minor grooves of two DNA gyres and the adjacent αN helix (30) and includes Tyr-41, a residue shown to regulate HP1α binding to heterochromatin (23). The stretch of residues (positions 36–58) forming the interaction interface is shown in Fig. 5 mapped onto a ribbon diagram of the nucleosome (30). There are no significant perturbations elsewhere in the H3(1–59) sequence.

DISCUSSION

Our results confirm and extend previous reports (22, 23) that CSDα plays a role in histone H3 recognition. This interaction is distinct from the well studied CD-mediated interaction of HP1 with methylated H3K9. We have shown by NMR and CSDα mutagenesis that H3(1–59) interacts with CSDα through a run of residues, H3(36–58), containing a P*x*V*x*L-related motif, ^{43}PGTVAL^{48}, in a manner very similar to that of CAF1 p150, a known P*x*V*x*L-containing family member (24). Mutation of Val-46 in this motif to alanine significantly decreases the strength of the interaction with HP1α (22). Structural studies of the interaction of the highly homologous CSDβ with the CAF1 P*x*V*x*L peptide suggest that an exact consensus is not required for interaction (24, 25). The deviation from the consensus in the H3 P*x*V*x*L-like sequence probably accounts for the reduced affinity of the H3 peptide (K_D 58 μM) relative to the CAF1 peptide (K_D 0.43 μM). The CSDα interaction with H3(36–58) provides a rationale for the *in vivo* observations that phosphorylation of Tyr-41 by JAK2 specifically displaces HP1α from chromatin and that HP1α binding to chromatin can be competed in permeabilized cells by the H3(31–56) peptide (23).

The region of H3 responsible for binding to CSDα, comprising residues 36–58, includes the αN helix, which is located near the nucleosomal DNA exit and entry point, and is an important regulator of nucleosome dynamics and stability (33). In the conventional representation of the static nucleosome, H3 residues 36–58 would be relatively inaccessible and confined within the DNA gyres (Fig. 5, *A* and *B*). Although a window of opportunity for HP1 binding *in vivo* may, of course, arise during DNA replication (34) or transcription, nucleosomes can also undergo spontaneous conformational changes that result in transient unwrapping of the DNA from the octamer surface (Fig. 5*C*) (35–37). Unwrapping may also be caused by the activity of remodeling complexes (38), and remodeling complexes (Brg1 (22) and ACF1 (39)) have been reported to facilitate HP1 loading onto chromatin. In addition, unwrapping might result from the action of a protein such as HMGB1, which binds to linker DNA adjacent to the nucleosome (and interacts with the H3 tail (40) and data not shown[4]) and could cause unwrapping of DNA by torsion transmitted from bending of the linker DNA (41). Moreover, the αN helical region of H3 in Mg^{2+}-condensed chromatin has been shown by hydrogen/deuterium

[4] M. Watson, H. Fischl, K. Stott, and J. O. Thomas, unpublished data.

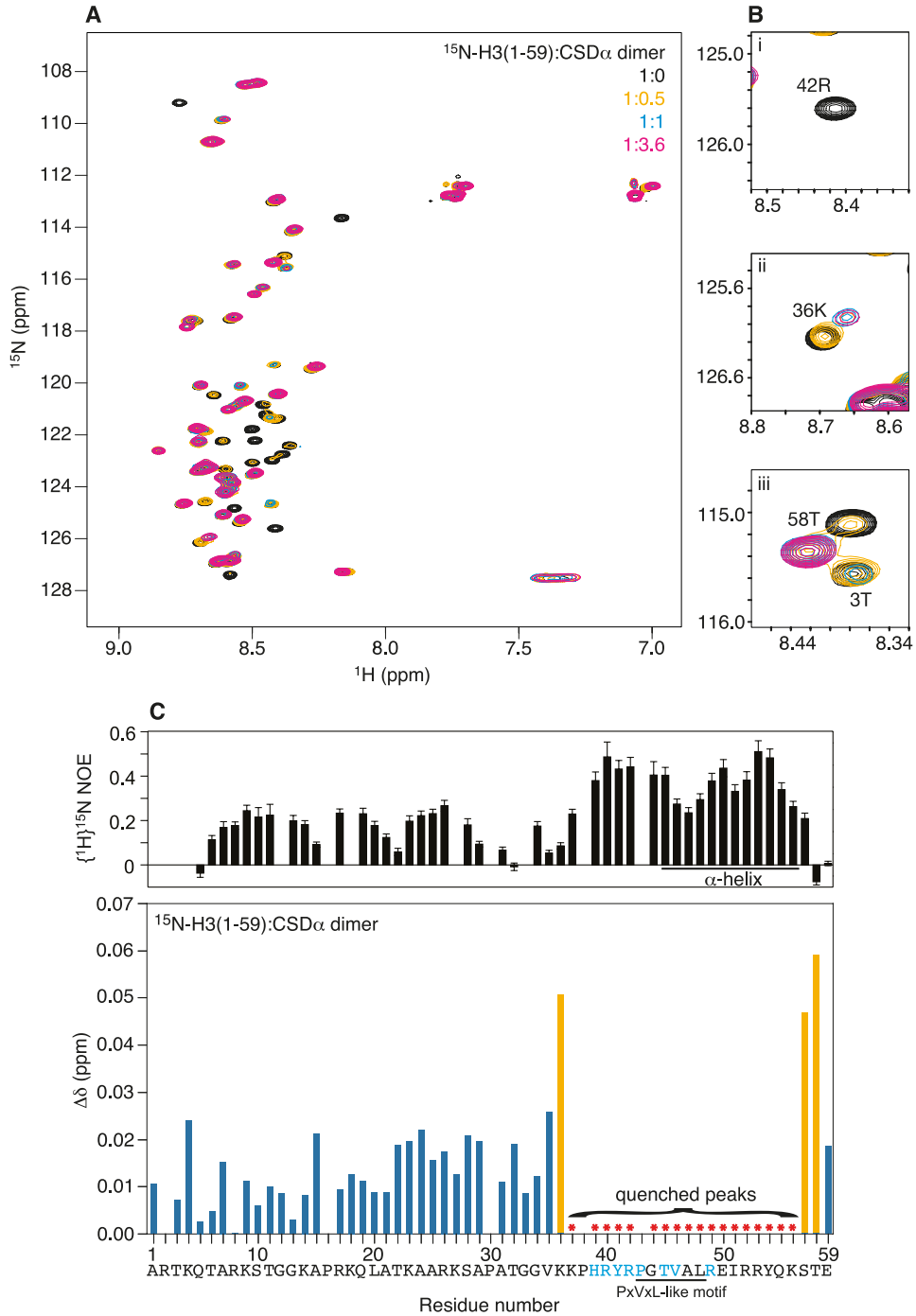

FIGURE 4. **Identification of CSDα-binding site on H3(1–59).** *A*, ^{15}N HSQC spectra of ^{15}N-labeled H3(1–59) alone and in the presence of CSDα at varying input ratios as indicated. *B*, expansions of spectra in *A* showing examples of different responses (peak disappearance (*panel i*) and peak shift (*panels ii* and *iii*)). *C*, chemical shift perturbation map showing the residues in the interacting region, with significantly shifting peaks (*yellow*) and peaks that broaden and disappear (*red asterisks*) highlighted. The H3(1–59) amino acid sequence is indicated below the *x axis*; residues known to make contacts with DNA (30) are shown in *light blue*. ^{15}N{^{1}H} heteronuclear NOE values are shown above to indicate the residues (positions 39–55) that display reduced flexibility/secondary structure in the free peptide; residues 45–56 (α-helix) constitute the αN helix in nucleosomal H3.

exchange studies to be relatively exposed (42), possibly as a result of structural rearrangement on chromatin folding. In contrast, residues 1–37, which are relatively exposed and flexible in soluble arrays, are protected to the same degree as the folded H3 "core" within the H3/H4 tetramer, suggesting that the N-terminal tail (and the H3K9 CD-binding site) is buried in the folded structure. Thus, at least in this form of condensed chromatin, the αN helical region might remain accessible to CSD-mediated interaction with HP1. The DNA that is unpeeled to allow access could then be captured by the basic interdomain HP1 linker, thereby stabilizing the complex. HP1 could thus prevent further spontaneous unwrapping while also preventing access of remodeling complexes (22, 38).

We suggest that HP1 contributes to repressive condensed chromatin structure in at least two ways: 1) CD tethering

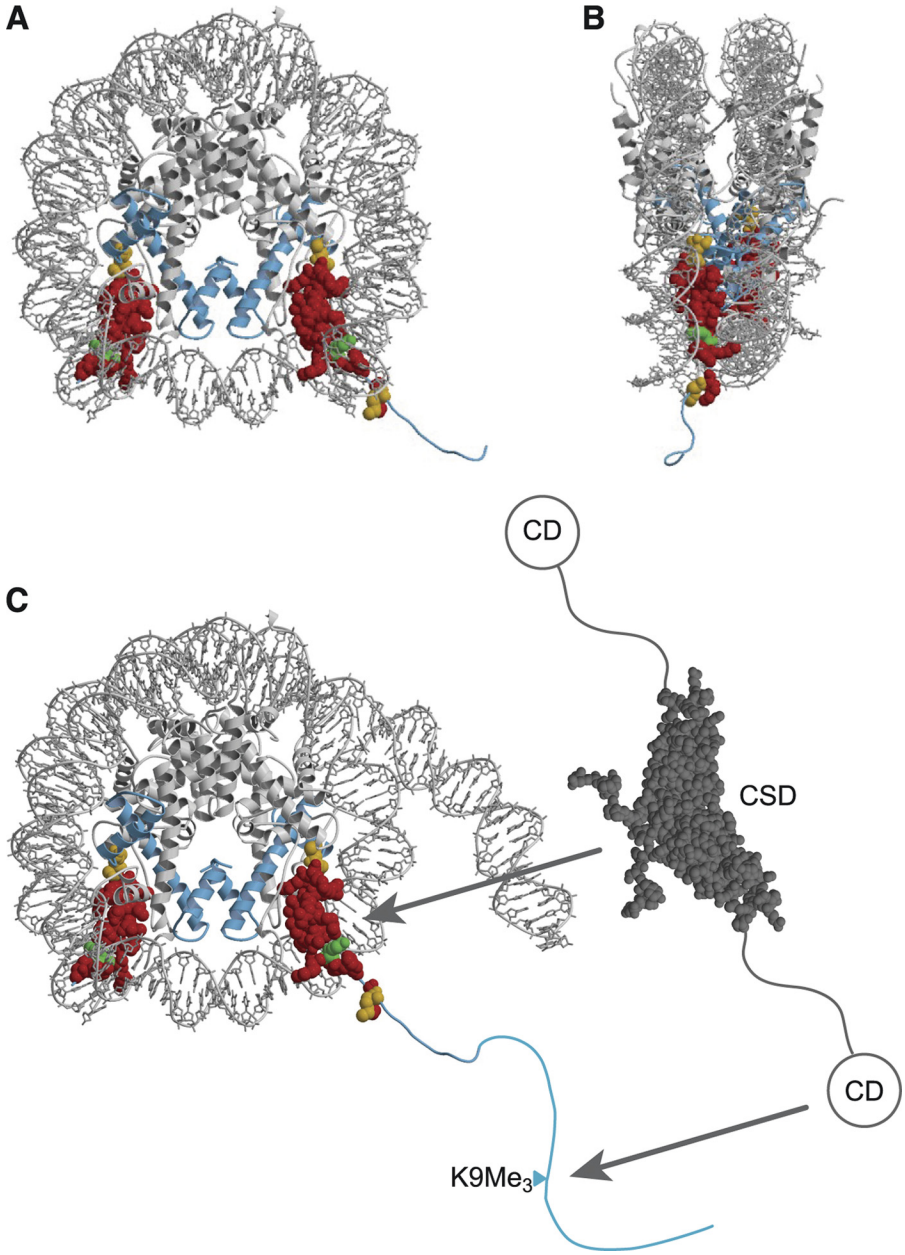

FIGURE 5. **CSDα-binding site on H3(1–59) shown in the context of the nucleosome.** *A*, space-filling representation of the H3 residues that are significantly shifted (*yellow*) or "quenched" (*red*) on addition of CSDα, mapped onto the nucleosome (Protein Data Bank code 1AOI (30)). Histone-fold helices of H3 are shown as *blue ribbons*, and H3Y41 is indicated in *green* space-filling representation. *B*, same as *A* after a 90° rotation about the vertical axis. *C*, bifunctional binding of an HP1 dimer to a single nucleosome, shown as in *A* except that the entering/exiting DNA strand lying over the CSDα-binding site is shown "unwrapped" to illustrate how conformational changes resulting from nucleosome dynamics may expose these residues. HP1 is shown schematically in *gray* with the CSD (Protein Data Bank code 1S4Z (24)) in space-filling representation. The H3 tail is extended beyond the density detected in the x-ray structure to include the methylated Lys-9 site (*K9Me$_3$*), which recruits the CD. Structural representations were prepared using MolScript (31) and Raster3D (32).

through methylated H3K9 with consequent recruitment of silencing complexes and 2) CSD binding to the H3 αN helix.

Acknowledgments—We thank Andy Bannister for plasmid pGEX2T-HP1CSDα(109–185) and Fred Northrop for technical assistance.

REFERENCES

1. Hediger, F., and Gasser, S. M. (2006) Heterochromatin protein 1: don't judge the book by its cover! *Curr. Opin. Genet. Dev.* **16,** 143–150
2. Fanti, L., and Pimpinelli, S. (2008) HP1: a functionally multifaceted protein. *Curr. Opin. Genet. Dev.* **18,** 169–174
3. Kwon, S. H., and Workman, J. L. (2011) The changing faces of HP1: from heterochromatin formation and gene silencing to euchromatic gene expression: HP1 acts as a positive regulator of transcription. *BioEssays* **33,** 280–289
4. Ayoub, N., Jeyasekharan, A. D., and Venkitaraman, A. R. (2009) Mobilization and recruitment of HP1: a bimodal response to DNA breakage. *Cell Cycle* **8,** 2945–2950
5. Cheutin, T., McNairn, A. J., Jenuwein, T., Gilbert, D. M., Singh, P. B., and Misteli, T. (2003) Maintenance of stable heterochromatin domains by dynamic HP1 binding. *Science* **299,** 721–725
6. Festenstein, R., Pagakis, S. N., Hiragami, K., Lyon, D., Verreault, A., Sekkali, B., and Kioussis, D. (2003) Modulation of heterochromatin protein 1

dynamics in primary mammalian cells. *Science* **299,** 719–721
7. Schmiedeberg, L., Weisshart, K., Diekmann, S., Meyer Zu Hoerste, G., and Hemmerich, P. (2004) High- and low-mobility populations of HP1 in heterochromatin of mammalian cells. *Mol. Biol. Cell* **15,** 2819–2833
8. Müller, K. P., Erdel, F., Caudron-Herger, M., Marth, C., Fodor, B. D., Richter, M., Scaranaro, M., Beaudouin, J., Wachsmuth, M., and Rippe, K. (2009) Multiscale analysis of dynamics and interactions of heterochromatin protein 1 by fluorescence fluctuation microscopy. *Biophys. J.* **97,** 2876–2885
9. Lachner, M., O'Carroll, D., Rea, S., Mechtler, K., and Jenuwein, T. (2001) Methylation of histone H3 lysine 9 creates a binding site for HP1 proteins. *Nature* **410,** 116–120
10. Bannister, A. J., Zegerman, P., Partridge, J. F., Miska, E. A., Thomas, J. O., Allshire, R. C., Kouzarides, T. (2001) Selective recognition of methylated lysine 9 on histone H3 by the HP1 chromodomain. *Nature* **410,** 120–124
11. Meehan, R. R., Kao, C. F., and Pennings, S. (2003) HP1 binding to native chromatin *in vitro* is determined by the hinge region and not by the chromodomain. *EMBO J.* **22,** 3164–3174
12. Lomberk, G., Wallrath, L., and Urrutia, R. (2006) The heterochromatin protein 1 family. *Genome Biol.* **7,** 228
13. Murzina, N., Verreault, A., Laue, E., and Stillman, B. (1999) Heterochromatin dynamics in mouse cells: interaction between chromatin assembly factor 1 and HP1 proteins. *Mol. Cell* **4,** 529–540
14. Smothers, J. F., and Henikoff, S. (2000) The HP1 chromoshadow domain binds a consensus peptide pentamer. *Curr. Biol.* **10,** 27–30
15. Ball, L. J., Murzina, N. V., Broadhurst, R. W., Raine, A. R., Archer, S. J., Stott, F. J., Murzin, A. G., Singh, P. B., Domaille, P. J., and Laue, E. D. (1997) Structure of the chromatin-binding (chromo) domain from mouse modifier protein 1. *EMBO J.* **16,** 2473–2481
16. Brasher, S. V., Smith, B. O., Fogh, R. H., Nietlispach, D., Thiru, A., Nielsen, P. R., Broadhurst, R. W., Ball, L. J., Murzina, N. V., and Laue, E. D. (2000) The structure of mouse HP1 suggests a unique mode of single peptide recognition by the shadow chromodomain dimer. *EMBO J.* **19,** 1587–1597
17. Wallrath, L. L., and Elgin, S. C. (1995) Position effect variegation in *Drosophila* is associated with an altered chromatin structure. *Genes Dev.* **9,** 1263–1277
18. Danzer, J. R., and Wallrath, L. L. (2004) Mechanisms of HP1-mediated gene silencing in *Drosophila*. *Development* **131,** 3571–3580
19. Fischle, W., Wang, Y., and Allis, C. D. (2003) Binary switches and modification cassettes in histone biology and beyond. *Nature* **425,** 475–479
20. Fan, J. Y., Rangasamy, D., Luger, K., and Tremethick, D. J. (2004) H2A.Z alters the nucleosome surface to promote HP1α-mediated chromatin fiber folding. *Mol. Cell* **16,** 655–661
21. Canzio, D., Chang, E. Y., Shankar, S., Kuchenbecker, K. M., Simon, M. D., Madhani, H. D., Narlikar, G. J., and Al-Sady, B. (2011) Chromodomain-mediated oligomerization of HP1 suggests a nucleosome-bridging mechanism for heterochromatin assembly. *Mol. Cell* **41,** 67–81
22. Lavigne, M., Eskeland, R., Azebi, S., Saint-André, V., Jang, S. M., Batsché, E., Fan, H. Y., Kingston, R. E., Imhof, A., and Muchardt, C. (2009) Interaction of HP1 and Brg1/Brm with the globular domain of histone H3 is required for HP1-mediated repression. *PLoS Genet.* **5,** e1000769
23. Dawson, M. A., Bannister, A. J., Göttgens, B., Foster, S. D., Bartke, T., Green, A. R., and Kouzarides, T. (2009) JAK2 phosphorylates histone H3Y41 and excludes HP1α from chromatin. *Nature* **461,** 819–822
24. Thiru, A., Nietlispach, D., Mott, H. R., Okuwaki, M., Lyon, D., Nielsen, P. R., Hirshberg, M., Verreault, A., Murzina, N. V., and Laue, E. D. (2004) Structural basis of HP1-P*x*V*x*L motif peptide interactions and HP1 localization to heterochromatin. *EMBO J.* **23,** 489–499
25. Huang, Y., Myers, M. P., and Xu, R. M. (2006) Crystal structure of the HP1-EMSY complex reveals an unusual mode of HP1 binding. *Structure* **14,** 703–712
26. Verreault, A., Kaufman, P. D., Kobayashi, R., and Stillman, B. (1998) Nucleosomal DNA regulates the core histone-binding subunit of the human Hat1 acetyltransferase. *Curr. Biol.* **8,** 96–108
27. Cavanagh, J., Fairbrother, W. J., Palmer, A. G., and Skelton, N. J. (1996) *Protein NMR Spectroscopy: Principles and Practice*, Academic Press, San Diego, CA
28. Vranken, W. F., Boucher, W., Stevens, T. J., Fogh, R. H., Pajon, A., Llinas, M., Ulrich, E. L., Markley, J. L., Ionides, J., and Laue, E. D. (2005) The CCPN data model for NMR spectroscopy: development of a software pipeline. *Proteins* **59,** 687–696
29. Zuiderweg, E. R. (2002) Mapping protein-protein interactions in solution by NMR spectroscopy. *Biochemistry* **41,** 1–7
30. Luger, K., Mäder, A. W., Richmond, R. K., Sargent, D. F., and Richmond, T. J. (1997) Crystal structure of the nucleosome core particle at 2.8 Å resolution. *Nature* **389,** 251–260
31. Kraulis, P. J. (1991) MOLSCRIPT—a program to produce both detailed and schematic plots of protein structures. *J. Appl. Crystallogr.* **24,** 946–950
32. Merritt, E. A., and Bacon, D. J. (1997) Raster3D: photorealistic molecular graphics. *Methods Enzymol.* **277,** 505–524
33. Ferreira, H., Somers, J., Webster, R., Flaus, A., and Owen-Hughes, T. (2007) Histone tails and the H3 αN helix regulate nucleosome mobility and stability. *Mol. Cell. Biol.* **27,** 4037–4048
34. Dialynas, G. K., Makatsori, D., Kourmouli, N., Theodoropoulos, P. A., McLean, K., Terjung, S., Singh, P. B., and Georgatos S. D. (2006) Methylation-independent binding to histone H3 and cell cycle-dependent incorporation of HP1β into heterochromatin. *J. Biol. Chem.* **281,** 14350–14360
35. Li, G., and Widom, J. (2004) Nucleosomes facilitate their own invasion. *Nat. Struct. Mol. Biol.* **11,** 763–769
36. Li, G., Levitus, M., Bustamante, C., and Widom, J. (2005) Rapid spontaneous accessibility of nucleosomal DNA. *Nat. Struct. Mol. Biol.* **12,** 46–53
37. Poirier, M. G., Bussiek, M., Langowski, J., and Widom, J. (2008) Spontaneous access to DNA target sites in folded chromatin fibers. *J. Mol. Biol.* **379,** 772–786
38. Somers, J., and Owen-Hughes, T. (2009) Mutations to the histone H3 αN region selectively alter the outcome of ATP-dependent nucleosome-remodeling reactions. *Nucleic Acids Res.* **37,** 2504–2513
39. Eskeland, R., Eberharter, A., and Imhof, A. (2007) HP1 binding to chromatin methylated at H3K9 is enhanced by auxiliary factors. *Mol. Cell. Biol.* **27,** 453–465
40. Ueda, T., Chou, H., Kawase, T., Shirakawa, H., and Yoshida, M. (2004) Acidic C-tail of HMGB1 is required for its target binding to nucleosome linker DNA and transcription stimulation. *Biochemistry* **43,** 9901–9908
41. Travers, A. A. (2003) Priming the nucleosome: a role for HMGB proteins? *EMBO Rep.* **4,** 131–136
42. Kato, H., Gruschus, J., Ghirlando, R., Tjandra, N., and Bai, Y. (2009) Characterization of the N-terminal tail domain of histone H3 in condensed nucleosome arrays by hydrogen exchange and NMR. *J. Am. Chem. Soc.* **131,** 15104–15105